HHS Public Access

Author manuscript

*Hepatology*. Author manuscript; available in PMC 2024 November 01.

Published in final edited form as:

*Hepatology*. 2023 November 01; 78(5): 1337–1351. doi:10.1097/HEP.0000000000000380.

# Antisense oligonucleotide silencing of a glycosyltransferase, *Poglut1*, improves the liver phenotypes in mouse models of Alagille syndrome

**Nima Niknejad**[1], **Duncan Fox**[1,2], **Jennifer L. Burwinkel**[3], **Neda Zarrin-Khameh**[4], **Soomin Cho**[5], **Armand Soriano**[6], **Ashley E. Cast**[3], **Mario F. Lopez**[1], **Kari A. Huppert**[3], **Frank Rigo**[6], **Stacey S. Huppert**[3,7], **Paymaan Jafar-Nejad**[6], **Hamed Jafar-Nejad**[1,2,5]

[1]Department of Molecular and Human Genetics, Baylor College of Medicine, Houston, TX

[2]Genetics & Genomics Graduate Program, Baylor College of Medicine, Houston, TX

[3]Division of Gastroenterology, Hepatology and Nutrition, Cincinnati Children's Hospital Medical Center, Cincinnati, OH

[4]Department of Pathology & Immunology, Baylor College of Medicine and Ben Taub Hospital, Houston, TX

[5]Development, Disease Models & Therapeutics Graduate Program, Baylor College of Medicine, Houston, TX

[6]Ionis Pharmaceuticals, Carlsbad, CA

[7]Department of Pediatrics, University of Cincinnati College of Medicine, Cincinnati, OH

## Abstract

**Background and Aims:** Paucity of intrahepatic bile ducts is caused by various etiologies and often leads to cholestatic liver disease. For example, in patients with Alagille syndrome (ALGS), which is a genetic disease primarily caused by mutations in *JAG1*, bile duct paucity often results in severe cholestasis and liver damage. However, no mechanism-based therapy exists to restore the biliary system in ALGS or other diseases associated with bile duct paucity. Based on previous genetic observations, we investigate whether postnatal knockdown of the glycosyltransferase gene

**Corresponding author:** Hamed Jafar-Nejad, M.D., Department of Molecular and Human Genetics, Baylor College of Medicine, One Baylor Plaza, Room 919E, BCM225, Houston, TX 77030. hamedj@bcm.edu.

**Author contributions:** N.N., P.J., S.S.H., and H.J.N. designed the experiments. A.S., P.J., and F.R. designed and developed ASO-1 and characterized the ASO in adult wild-type mice at Ionis Pharmaceuticals. M.F.L. supported all mouse experiments. N.N. performed the ASO injections, most of the phenotypic analysis, and all cell culture experiments. D.F. performed the ink injections along with imaging and quantification of the biliary tree. S.C. analyzed the effects of ASO on the satellite cells. N.Z.K. contributed to the generation and analysis of the H&E data. J.L.B, A.E.C., K.A.H and S.S.H. performed and analyzed the RNAscope and ASO immunostaining. N.N. and H.J.N. wrote the manuscript with input from other authors. H.J.N. supervised the project.

**Conflicts of interest:** Armand Soriano owns stock in and is employed by Ionis Pharmaceuticals. Frank Rigo owns stock in and is employed by and owns intellectual property rights in Ionis Pharmaceuticals. Paymaan Jafar-Nejad owns stock in and is employed by Ionis Pharmaceuticals. The other authors declare no conflicts.

Supporting Information
Supporting Materials and Methods
Supporting Figs. S1 and S2
Supporting Tables S1 and S2

*Poglut1* can improve the ALGS liver phenotypes in several mouse models generated by removing one copy of *Jag1* in the germline with or without reducing the gene dosage of *Sox9* in the liver.

**Approach and Results:** Using an antisense oligonucleotide (ASO) established in this study, we show that reducing *Poglut1* levels in postnatal livers of ALGS mouse models with moderate to profound biliary abnormalities can significantly improve bile duct development and biliary tree formation. Importantly, ASO injections prevent liver damage in these models without adverse effects. Furthermore, ASO-mediated *Poglut1* knockdown improves biliary tree formation in a different mouse model with no *Jag1* mutations. Cell-based signaling assays indicate that reducing POGLUT1 levels or mutating POGLUT1 modification sites on JAG1 increase JAG1 protein level and JAG1-mediated signaling, suggesting a likely mechanism for the observed *in vivo* rescue.

**Conclusions:** Our preclinical studies establish ASO-mediated *POGLUT1* knockdown as a potential therapeutic strategy for ALGS liver disease and possibly other diseases associated with BD paucity.

## Graphical Abstract

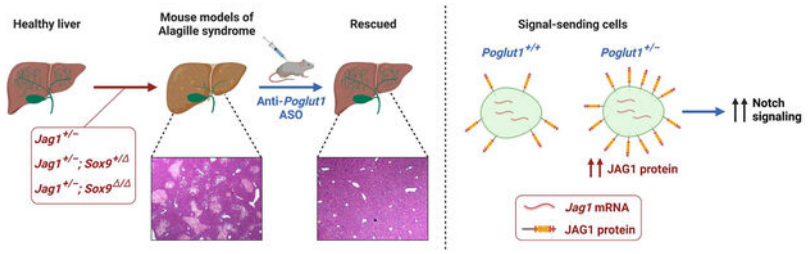


### Keywords

JAG1; biliary tree; Notch signaling; preclinical study; cholestasis

## Introduction

Alagille syndrome (ALGS) is a multisystem developmental disorder involving the liver, cardiovascular system, kidney, and skeletal system among other organs.[1,2] ALGS is caused by autosomal dominant mutations in *JAG1* (95%) or *NOTCH2* (2–3%), which encode key components of the Notch signaling pathway.[3–8] The characteristic feature of ALGS is intrahepatic bile duct (BD) paucity, defined as a significant decrease in the average number of BD per portal vein (PV).[2] BD paucity results in severe cholestasis in many ALGS patients and often leads to end-stage liver disease.

With an estimated frequency of 1:30,000, ALGS is the most common genetic disease resulting in intrahepatic cholestasis.[9] Standard of clinical care for BD paucity is directed towards reducing intrahepatic bile accumulation by altering the flow through surgery or modifying the enterohepatic bile acid transport through inhibitors and binding resins.[10,11] However, similar to other diseases associated with severe BD paucity, the only cure for the liver disease in ALGS is liver transplantation.[11] The shortage of suitable liver donors and the rather long time that patients usually spend on the liver transplant wait list highlight the need for identifying strategies to bypass the requirement for liver transplantation.

A recent study followed 293 ALGS patients who showed features of cholestasis by the age of 5 and had their native liver at the time of enrollment.[12] Prospective analysis of these patients showed that only 24% of them survived to age 18.5 without a liver transplant. This work, which is the largest multi-center natural history study of the ALGS liver disease to date, also reported that ALGS patients exhibit a second wave of liver disease due to fibrosis and portal hypertension in later childhood.[11,12] A more recent multicenter retrospective study analyzed the natural history of the disease in 1,433 patients who were confirmed to have ALGS.[13] In the 1,184 patients who had a history of neonatal cholestasis, a native liver survival rate of 40.3% at 18 years of age was reported.[13] Moreover, 68.9% of patients developed clinically evident portal hypertension by 18.[13] Together, these studies established that the burden of the liver disease and the need for transplantation is very high in ALGS patients.

We previously reported that on a pure C57BL/6 background, mice heterozygous for *Jag1* (*Jag1*$^{+/-}$) are a genetically representative model for ALGS and are born with significant BD paucity.[14] The BD paucity remains at postnatal day 30 (P30) and is accompanied by ductular reactions, hepatocyte necrosis and fibrosis, resembling chronic hepatobiliary disease.[14,15] We used this model to identify two dosage-sensitive genetic modifiers of the *Jag1*$^{+/-}$ phenotypes. First, we showed that the *Jag1*$^{+/-}$ BD paucity can be significantly improved by removing one copy of a glycosyltransferase called "protein *O*-glucosyltransferase 1" (*Poglut1*).[14] More recently, we reported that the *Jag1*$^{+/-}$ liver phenotypes are highly sensitive to the level of *Sox9* and established two additional ALGS models (*Jag1*$^{+/-}$;*Sox9*$^{+/flox}$;*Albumin-Cre* [hereafter called *Jag1*$^{+/-}$;*Sox9*$^{+/\Delta}$] and *Jag1*$^{+/-}$;*Sox9*$^{flox/flox}$;*Albumin-Cre* [hereafter called *Jag1*$^{+/-}$;*Sox9*$^{\Delta/\Delta}$]).[15] The BD paucity in these models is more severe than the *Jag1*$^{+/-}$ model and does not show improvement with age.[15] Therefore, these three models represent the broad range of liver phenotypes observed in ALGS patients.

Here we established an antisense oligonucleotide (ASO) which can efficiently knockdown (KD) *Poglut1 in vivo*, and found that it improves the liver phenotypes of all three models upon postnatal injection. Cell-based signaling assays suggest that reducing *Poglut1* level improves JAG1-mediated signaling by directly affecting JAG1 protein level and signaling. Our data suggest that ASO-mediated KD of *POGLUT1* might be a viable therapeutic strategy for ALGS liver disease.

## Materials and Methods

### ASO-1

The anti-*Poglut1* ASO (ASO-1; designed and developed by Ionis Pharmaceuticals) is a 3-10-3 cEt-ASO ($G_ST_ST_S$ **$^{m}C_SA_ST_SA_SA_ST_ST_S$** **$^{m}C_ST_S$** **$^{m}C_S$** $^{m}C_SA_SA$) with full phosphorothioate linkages (PS; "$_S$" subscripts in the sequence) and methylated cytosines ($^{m}C$). ASO-1 working stocks (5 mg/mL) were diluted in sterile PBS without calcium chloride and without magnesium chloride. Mice were subcutaneously injected with 50 mg/kg of ASO-1 or the same volume of PBS as control.

### Mouse strains and breeding

The following strains were used: WT C57BL/6, *Jag1*$^{dDSL}$ (*Jag1*$^{+/-}$)[14,16], *Albumin-Cre* (Jackson Laboratory #003574)[17], *Poglut1*$^{+/-}$ (*Poglut1*$^{+/GT(IST10323G11)TIGM}$)[18], and *Sox9*$^{flox/flox}$ (Jackson Laboratory #013106).[19] Animals were kept on a C57BL/6 background for all crosses. All animals were maintained in a temperature-controlled environment at 21°C with 12 hour light-dark cycles in a barrier facility at Baylor College of Medicine per Institutional Animal Care and Use Committee guidelines and under approved animal protocols. Litters were randomly assigned to PBS or ASO-1 injection groups, and all pups from the same litter were injected with either PBS or ASO-1.

### Quantification of the BD/PV ratio and fibrosis

The BD/PV ratio and fibrosis were quantified as previously described.[15,20] For details, please see Supporting Materials and Methods.

### RNAscope

Liver tissue was fixed overnight to 3 days at 4°C in 4% paraformaldehyde, washed with PBS, equilibrated in 30% sucrose PBS solution for cryoprotection, embedded in O.C.T. (Tissue-Tek®), and stored at −80°C. RNAscope was performed according to ACDbio Multiplex Fluorescent v2 Manual with some modifications. For details, please see Supporting Materials and Methods.

### Biliary tree ink injection and quantification of the biliary tree density

Retrograde biliary ink injection was performed as previously described.[21] After clearing, the liver lobes were imaged using a Ziess Axio Zoom.V16 microscope at 20x and reconstructed in Adobe Illustrator. For quantification of the biliary tree density, portions consisting of approximately one third of each left lobe were cropped from the whole image. Using the color threshold tool in ImageJ, each background was filtered out and ink areas were quantified.

### Cell culture and Notch signaling assay

Signal-receiving MEFs or COS7 cells were seeded in 24-well plates $8\times10^4$ cells/well and cotransfected with the TP-1 luciferase Notch-signaling reporter construct (0.12 μg/well), plasmids expressing WT mouse *Notch1* or *Notch2* or empty pcDNA3 (0.1 μg/well), and gWIZ β-galactosidase construct (0.06 μg/well). The latter was used for transfection efficiency normalization using HD-FuGENE (Promega, Cat. #E5911) according to the manufacturer's instructions. After 24 hours, media was removed and signal-sending HEK293T cells (or MEFs) stably expressing JAG1 ($1.5\times10^5$ cells/well in 1 mL medium) were overlaid on transfected MEFs (or COS7 cells, when MEFs were the signal-sending cells). After 24 hours of co-culture, cells were lysed and luciferase and β-galactosidase assays (Luciferase Assay System; Promega) were performed according to the manufacturer's instructions. Given the variability in luciferase-based co-culture assays, for each dataset, 3–4 independent experiments were performed, each comprised of 9 samples. For details, please see Supporting Materials and Methods.

### Statistical analysis

Analysis of body weights, BD/PV ratios, serum total bilirubin levels, necrosis and fibrosis was carried out with unpaired t-test, t-tests with Welch's correction, or one-way analysis of variance (ANOVA) with the appropriate multiple comparisons tests (Tukey's or Dunnett's) using Prism (GraphPad).

## Results

### Subcutaneous injection of ASO-1 can efficiently KD *Poglut1* in adult mouse livers with no liver toxicity

Our previous work indicated that removing one copy of *Poglut1* in the germline or with *Albumin-Cre* or *SM22α-Cre* leads to a significant improvement in *Jag1*$^{+/-}$ liver phenotypes.[14] Since both of these transgenes start CRE-mediated deletion in mouse embryos,[17,22] it was not clear whether decreasing *Poglut1* levels after birth would improve their biliary phenotype. To test this notion, which is a prerequisite for therapeutic targeting of *POGLUT1* in patients with ALGS, we identified a constrained ethyl (cEt) gapmer anti-*Poglut1* ASO (ASO-1) from a cell-based screen. Five weekly subcutaneous injections of ASO-1 at 50 mg/kg/dose into adult (8-week-old) WT mice led to ~95% *Poglut1* KD in the liver (Supporting Fig. S1, A and B). Despite efficient *Poglut1* KD, the animals did not show growth retardation (Supporting Fig. S1C) or statistically significant abnormalities in liver weight, AST, ALT, or bilirubin (Supporting Fig. S1, D and E). Therefore, we used this anti-*Poglut1* ASO for our rescue experiments.

### ASO-mediated *Poglut1* KD partially rescues the biliary abnormalities in P12 *Jag1*$^{+/-}$ animals

Based on the strong KD observed with five weekly doses of ASO-1 and because of the robust improvement in the *Jag1*$^{+/-}$ phenotype upon genetic removal of one copy (50%) of *Poglut1*,[14] we used two subcutaneous injections of ASO-1 at P1 and P7 (Fig. 1A). This injection regimen led to 46% and 58% reduction in *Poglut1* mRNA levels in *Jag1*$^{+/-}$ and WT livers, respectively, compared to PBS-injected controls (Fig. 1B).

To examine the expression pattern of *Poglut1* in the liver and assess the ability of the ASO to KD *Poglut1* in specific liver cell types, we performed RNAscope studies[23] on P12 livers. *Poglut1* is expressed in hepatocytes, biliary cells (*Sox9*$^{+}$), and periportal mesenchymal cells (*Jag1*$^{+}$, *Sox9*$^{-}$) (Fig. 1C). Visual inspection of RNAscope images suggests that *Poglut1* transcript levels are reduced in parenchymal and periportal regions of ASO-injected livers compared to control livers (Fig. 1C). We next quantified the *Poglut1*$^{+}$ pixel area within liver sections and calculated the relative area of the liver covered by *Poglut1* transcript signal (after excluding the PV and BD lumens and regions within the image without cells from the total area analyzed). This analysis showed that ASO injections reduce the *Poglut1*$^{+}$ area by ~51% in the parenchymal areas, which is an indication of KD in hepatocytes (Fig. 1D). A similar analysis on PV regions to primarily assess KD in the biliary and periportal mesenchymal cells showed a 37% reduction in *Poglut1*$^{+}$ area upon ASO injections (Fig. 1D). Antibody staining on PBS-injected and ASO-injected P12 WT livers showed broad ASO uptake by hepatocytes and portal mesenchymal cells (αSMA$^{+}$), but only limited signal

in biliary cells ($OPN^+$) (Fig. 1E). Together, these observations indicate that the cEt ASO used in our studies can efficiently target hepatocytes and periportal mesenchymal cells and potentially the biliary cells to a lesser extent.

Control *Jag1*$^{+/-}$ animals (PBS-injected) showed a qualitative reduction in the number of patent BDs around PVs, accompanied by weak αSMA staining in the PV mesenchyme and aberrant cytokeratin (CK)-expressing cells and hypercellularity in the liver parenchyma, suggestive of ductular reactions (Fig. 1F).[14,15] Quantification of the patent BDs for each genotype showed that in agreement with our previous reports at P3, P7 and P30,[14,15] the BD to PV ratio is significantly decreased in P12 *Jag1*$^{+/-}$ livers (PBS-injected) compared to WT controls (Fig. 1G). Importantly, ASO injections improved all of these phenotypes in *Jag1*$^{+/-}$ mice (Fig 1, F and G), suggesting that postnatal *Poglut1* KD can reverse the BD paucity present in late embryonic and early postnatal *Jag1*$^{+/-}$ animals and reduce the ductular reactions resulting from BD paucity in these animals.

## *Poglut1* KD in early postnatal period improves biliary development and significantly decreases liver damage in P30 *Jag1*$^{+/-}$ mice

By P30, *Jag1*$^{+/-}$ animals exhibit more severe ductular reactions and also some degree of necrosis.[14] To examine whether the ASO-induced improvements observed in P12 *Jag1*$^{+/-}$ livers persist until a later stage, we analyzed additional cohorts of *Jag1*$^{+/-}$ mice and their WT siblings injected with the same ASO or PBS regimen as P12 (Fig. 2A). Similar to P12 livers, the ASO significantly reduced *Poglut1* mRNA levels in WT (62%) and *Jag1*$^{+/-}$ (58%) livers (Fig. 2B). Two injections of ASO-1 led to a statistically significant increase in the BD to PV ratio in P30 *Jag1*$^{+/-}$ mice, accompanied by a strong reduction in ductular reactions and periportal hypercellularity and a statistically significant rescue of liver necrosis and fibrosis in these animals (Fig. 2, C–H). These data provide strong evidence that a sustained improvement in *Jag1*$^{+/-}$ liver phenotypes can be achieved by a limited number of anti-*Poglut1* ASO injections.

## *Poglut1* KD in early postnatal period improves biliary development and prevents liver damage in ALGS mouse models with severe liver phenotypes

Similar to *Jag1*$^{+/-}$ animals, two injections of ASO-1 resulted in a sustained significant reduction in liver *Poglut1* mRNA levels in models with more severe liver phenotypes (*Jag1*$^{+/-}$;*Sox9*$^{+/\Delta}$ and *Jag1*$^{+/-}$;*Sox9*$^{\Delta/\Delta}$) (Figs. 3A and 4A; 72% reduction in *Jag1*$^{+/-}$;*Sox9*$^{+/\Delta}$ and 66% reduction in *Jag1*$^{+/-}$;*Sox9*$^{\Delta/\Delta}$). In both genotypes, ASO injections led to a significant increase in the BD to PV ratio (Figs. 3B and 4B). In agreement with our recent report,[15] the average BD to PV ratio in PBS-injected P30 *Jag1*$^{+/-}$;*Sox9*$^{+/\Delta}$ and *Jag1*$^{+/-}$;*Sox9*$^{\Delta/\Delta}$ animals was lower than that in *Jag1*$^{+/-}$ mice (Figs. 3B and 4B; compare to Fig. 2C). Nevertheless, upon ASO injections, the average BD to PV ratio rose to the same level as ASO-injected *Jag1*$^{+/-}$ livers or even higher. These observations suggest that ASO-mediated *Poglut1* KD can improve biliary development in ALGS mouse models regardless of the severity of the phenotype.

At P30, *Jag1*$^{+/-}$;*Sox9*$^{+/\Delta}$ and *Jag1*$^{+/-}$;*Sox9*$^{\Delta/\Delta}$ animals show rather severe ductular reactions, accompanied by hypercellularity in the liver parenchyma, fibrosis and extensive necrosis

(Figs. 3 and 4).[15] ASO injections dramatically improved these phenotypes, including a full rescue of necrosis (Fig. 3, C–G and Fig. 4, C–G). These phenotypic improvements were accompanied by a significant increase in the average body weight and a significant reduction in the serum total bilirubin of both genotypes (Fig. 3, H and I, and Fig. 4, H and I). We conclude that two postnatal injections of an anti-*Poglut1* ASO can significantly improve the severe liver phenotypes observed in these two ALGS models.

## ASO-1 dramatically improves the biliary tree structure in ALGS models

Using retrograde ink injections into the common BD, we have previously reported that the biliary tree fails to extend to the liver periphery in P30 $Jag1^{+/-}$ animals and that this phenotype is worsened upon removing one copy of *Sox9* in the liver.[15] In agreement with this report, P30 PBS-injected $Jag1^{+/-}$ and $Jag1^{+/-};Sox9^{+/\Delta}$ animals showed a stepwise reduction in the degree of biliary tree extension towards liver periphery compared to PBS-injected WT animals (Fig. 5A). Furthermore, ink injections showed a rudimentary biliary tree in PBS-injected $Jag1^{+/-};Sox9^{\Delta/\Delta}$ animals, mostly limited to the hilar region of the liver (Fig. 5A). Similarly, quantification of the area of the liver covered by the biliary tree indicated a stepwise reduction in biliary density in $Jag1^{+/-}$ and the other two models (Fig. 5B). Our two-dose ASO regimen did not cause any biliary tree abnormalities in WT animals (Fig. 5, A and B). However, the ASO led to biliary tree augmentation in all three models (Fig. 5, A and B). In the two severe models, ASO injections led to a remarkable improvement in the extension of the biliary tree towards the liver lobe periphery and the density of biliary tree coverage in the liver (Fig. 5, A and B). These data reveal the beneficial effects of *Poglut1* KD in promoting biliary tree development in ALGS mouse models.

Analysis of liver sections from mice with conditional loss of *Sox9* in the liver with albumin/α-fetoprotein-Cre (*Alfp-Cre*) was reported to cause a delay in BD morphogenesis, which fully resolved by five weeks of age.[24] In the course of our ink injection studies, we noticed a mild but statistically significant reduction in the biliary tree density of $Albumin\text{-}Cre;Sox9^{flox/flox}$ animals (Fig. 5, C and D; $Jag1^{+/+};Sox9^{\Delta/\Delta}$). Notably, the anti-*Poglut1* ASO rescued this phenotype as well, suggesting that the biliary tree enhancement caused by *Poglut1* KD is not limited to animals lacking one copy of *Jag1*.

## The ASO induces significant *Poglut1* KD in the muscle but does not reduce the number of muscle stem cells

We have reported that recessive missense mutations in *POGLUT1* cause a form of limb-girdle muscular dystrophy in human patients called LGMD R21 (OMIM #617232; also called LGMD 2Z).[25,26] Biochemical experiments indicate that these mutations generally result in an 80–85% decrease in POGLUT1's enzymatic activity.[25,26] Analysis of patient muscle samples showed reduced NOTCH1 signaling and a severe decrease in the number of $PAX7^+$ muscle stem cells (satellite cells).[25,26] $Poglut1^{+/-}$ mice do not exhibit any gross morphological defects and growth abnormalities,[14,18] suggesting that removing one copy of *Poglut1* does not affect muscle development and function. Nevertheless, to establish ASO-mediated *Poglut1* KD as a therapeutic strategy in ALGS, it is important to demonstrate that the rescue of ALGS liver phenotypes in *Jag1*-haploinsufficient animals upon ASO-mediated *Poglut1* KD is not accompanied by a reduction in the number of $PAX7^+$ satellite

cells. As shown in Supporting Fig. S2A, two injections of ASO-1 resulted in a significant decrease in *Poglut1* mRNA levels in quadriceps muscles. However, staining of quadriceps muscle sections of P30 animals indicated that a comparable number of $PAX7^{+}$ cells are present in ASO-injected versus PBS-injected WT and $Jag1^{+/-}$ animals (Supporting Fig. S2, B and C). These data suggest that *Poglut1* KD by systemic injection of a cEt ASO does not reduce the number of satellite cells in WT or $Jag1^{+/-}$ mice.

## POGLUT1 negatively regulates JAG1 protein level and JAG1-mediated signaling

To elucidate the effects of reducing *Poglut1* levels on JAG1, we generated WT and $Poglut1^{+/-}$ mouse embryonic fibroblasts (MEFs) and stably infected them with a tetracycline-inducible human *JAG1* transgene (*tet-JAG1*). Treating WT-*tet-JAG1* MEFs with doxycycline led to accumulation of JAG1 protein and a robust induction of endogenous NOTCH1 signaling in these cells (Fig. 6A). Treating $Poglut1^{+/-}$-*tet-JAG1* MEFs with doxycycline led to the induction human *JAG1* mRNA at levels comparable to those seen in WT-*tet-JAG1* MEFs (Fig. 6B). However, the levels of human JAG1 protein and endogenous N1-ICD were higher in $Poglut1^{+/-}$ MEFs compared to WT MEFs (Fig. 6A), indicating that loss of one copy of *Poglut1* in MEFs increases JAG1 protein level and NOTCH1 activation.

Since both JAG1 and NOTCH receptors are glycosylated by POGLUT1,[14,18,27] the increased NOTCH1 activation observed in $Poglut1^{+/-}$ cells can theoretically result from the effects of *Poglut1* heterozygosity in signal-receiving or signal-sending cells (or both). To address this issue, we performed co-culture assays between MEFs (WT or $Poglut1^{+/-}$) and another cell type (COS7 or HEK293T, both $POGLUT1^{+/+}$) and used luciferase activity driven by a Notch-responsive reporter (TP1–1-luc)[28] as the readout for Notch signaling. Induction of JAG1 expression in WT-*tet-JAG1* MEFs led to ~2-fold increase in NOTCH1-mediated signaling and ~4-fold increase in NOTCH2-mediated signaling in COS7 cells compared to parallel co-cultures without JAG1 induction (Fig. 6C; black bars). $Poglut1^{+/-}$-*tet-JAG1* MEFs were able to induce significantly more NOTCH1 and NOTCH2-mediated signaling compared to WT-*tet-JAG1* MEFs (Fig. 6C; gray bars), indicating that reducing *Poglut1* levels in signal-sending cells can increase the ability of JAG1 to activate NOTCH receptors in neighboring cells.

In reciprocal experiments, we used MEFs as signal-receiving cells and cultured them with $POGLUT1^{+/+}$-*tet-JAG1* HEK293T cells. Induction of JAG1 in HEK293T cells induced a 5–6-fold increase in NOTCH1 and NOTCH2 signaling in WT MEFs compared to parallel co-cultures without JAG1 induction (Fig. 6D). Removing one copy of *Poglut1* in signal-receiving MEFs led to a statistically significant decrease in JAG1-mediated NOTCH1 and NOTCH2 signaling (Fig. 6D). These experiments indicate that decreasing *Poglut1* in signal-receiving cells leads to a reduction in NOTCH1 and NOTCH2 signaling upon receptor overexpression. We also co-cultured $POGLUT1^{+/+}$-*tet-JAG1* HEK293T cells with MEFs transfected with empty pcDNA3 vector to assess the impact of decreasing *Poglut1* expression level on signaling by endogenous NOTCH receptors. JAG1 from HEK293T cells led to a 2-fold increase in signaling mediated by endogenous NOTCH receptors in WT MEFs (Fig. 6D). Reducing one copy of *Poglut1* in signal-receiving MEFs did not lead to a significant reduction in JAG1-mediated Notch signaling in these cells (Fig. 6D).

Together, these experiments indicate that *Poglut1* heterozygosity in signal-receiving and signal-sending cells affects JAG1-Notch signaling in opposite directions.

JAG1 has four POGLUT1 modifications sites (Fig. 6E), all of which are efficiently *O*-glucosylated by POGLUT1.[14] To examine the role of JAG1 *O*-glucosylation in Notch signaling, we generated *Poglut1*$^{+/+}$ MEFs stably infected with tetracycline-inducible human *JAG1* transgenes harboring point mutations that abolish *O*-glucosylation in individual POGLUT1 modification sites or in all four. We found that loss of *O*-glucosylation sites on JAG1 recapitulates the effects of *Poglut1* heterozygosity on JAG1 protein level and on JAG1's ability to induce NOTCH1 and NOTCH2 signaling (Fig. 6, F and G). These experiments strongly suggest that reducing the POGLUT1-mediated glycosylation of JAG1 increases the JAG1 protein level and the ability of JAG1 to induce Notch signaling in neighboring cells.

## Discussion

Intrahepatic BD paucity can result from various etiologies, including genetic, infectious, nutritional and endocrine.[29] BD paucity commonly leads to cholestatic liver disease and often impacts the liver function severely enough to require liver transplantation.[29] Other than liver transplant, the standard of care for BD paucity is mostly geared toward symptomatic relief, although the recent approval of ileal bile acid transporter (IBAT) inhibitors for clinical use in ALGS and progressive familial intrahepatic cholestasis (PFIC) has been a major advance in improving the course of disease and quality of life in patients.[10,30,31] Nevertheless, no approved mechanism-based strategy exists to enhance the intrahepatic biliary tree formation. Here, we report that two injections of an anti-*Poglut1* ASO during the early postnatal period lead to a statistically significant improvement in the BD to PV ratio and the assessed clinical and pathologic criteria in all three models of the ALGS liver disease examined in this study. *Jag1*$^{+/-}$ animals already show a dramatic reduction in the number of SOX9$^{+}$ biliary cells at embryonic day 18, a lack of patent BDs in the peripheral areas of the liver at P0, and a significant decrease in BD to PV ratio as early as P3.[14,15] Therefore, our ASO injection regimen starts when the animals already show BD paucity. The BD to PV ratio is not fully rescued by the ASO. Nevertheless, ASO treatment results in a strong reduction in the degree of ductular reactions and periportal inflammation, dramatically improves the biliary tree structure—both the degree of extension toward liver periphery and the density of the tree—and almost completely prevents the appearance of the liver damage response in ALGS models, as evidenced by the rescue of fibrosis, necrosis and bilirubin levels. These observations suggest that ASO-mediated reduction of *POGLUT1* in the liver of ALGS patients might have the potential to improve their BD paucity enough to avert the need for liver transplantation.

As shown here and previously,[14,15] there is a negative correlation between the level of SOX9 in hepatobiliary cells and the severity of ALGS liver phenotypes in our mouse models and in human patients. In addition, a recent study reported that a small molecule with putative Notch activating properties can induce the expression of *Sox9b* and rescue the liver phenotypes in a zebrafish model of ALGS.[32] Lastly, *Sox9* has been shown to be a direct target of JAG1-Notch signaling in hepatoblasts.[33]Accordingly, we expected that

ASO-mediated *Poglut1* KD will improve the $Jag1^{+/-}$ liver phenotypes in a SOX9-dependent manner. Rather surprisingly, not only wasn't this the case, but ASO injections led to a stronger rescue of the liver phenotypes in $Jag1^{+/-};Sox9^{+/\Delta}$ and especially $Jag1^{+/-};Sox9^{\Delta/\Delta}$ animals compared to the original $Jag1^{+/-}$ model. These data indicate that expression of SOX9 in biliary cells is not essential for the improvement of *Jag1*-haploinsufficient liver phenotypes by anti-*Poglut1* ASO. This conclusion is in agreement with the observation that ASO injections also rescue the mild biliary tree defects caused by conditional loss of *Sox9* in the liver. Given the transient and redundant role played by SOX9 in BD development,[24,34] a likely explanation is that upon enhanced JAG1-mediated signaling caused by *Poglut1* KD, Notch pathway targets other than SOX9 are induced in biliary cells and lead to SOX9-independent rescue of the phenotypes. Regardless of the mechanism, our data suggest that the beneficial effects of *Poglut1* KD on postnatal biliary development are not limited to a *Jag1*-haploinsufficient context. How can reducing SOX9 make the $Jag1^{+/-}$ phenotype worse but paradoxically improve the therapeutic response to *Poglut1* KD? It has recently been reported that biliary cells express SOX9 at variable levels and that the transcriptomes of $SOX9^{low}$ and $SOX9^{high}$ biliary cells are quite distinct from each other,[35] providing a potential mechanism for our observation which awaits experimental verification.

Experiments on *Poglut1*-mutant *Drosophila* (official gene name: *rumi*), *Poglut1* KD *Drosophila* S2 cells, $Poglut1^{-/-}$ mice, several *Poglut1* KD mammalian cells, and muscle samples from LGMD R21 patients have indicated that POGLUT1 promotes the activation of *Drosophila* Notch and mammalian NOTCH1.[18,25,26,36,37] Moreover, the current work indicates that removing one copy of *Poglut1* in signal-receiving MEFs reduces the activation of overexpressed NOTCH1 and NOTCH2 by JAG1 from neighboring cells. Given our previous report that mutating the *O*-glucosylation sites of Notch in transgenic *Drosophila* phenocopies the effects of loss of *Poglut1*on Notch signaling,[37] these observations suggest that reducing Notch *O*-glucosylation leads to reduced Notch activation. However, the improvements in $Jag1^{+/-}$ liver phenotypes upon genetic [14] and ASO-mediated (this study) reduction in *Poglut1* suggest that POGLUT1 reduces JAG1-mediated Notch signaling. Moreover, similar to *Poglut1* heterozygosity, mutating the POGLUT1 targets sites on JAG1 is associated with an increase in JAG1 protein level and signaling ability, strongly suggesting that reducing JAG1 *O*-glucosylation leads to increased JAG1-mediated Notch activation. Accordingly, we suggest that the opposite effects of reducing *Poglut1* in signal-receiving versus signal-sending cells on Notch pathway activation can be explained by differential roles played by *O*-glucose residues on NOTCH1 and NOTCH2 versus JAG1, although we cannot exclude that an increase in the level of endogenous JAG1 in $Poglut1^{+/-}$ signal-receiving cells reduces NOTCH1/2 signaling via *cis*-inhibition.[38] Importantly, when JAG1 was overexpressed in a monoculture of $Poglut1^{+/-}$ MEFs, endogenous NOTCH1 activation was increased, not decreased (Fig. 6A). Altogether, our data suggest that the effect *Poglut1* reduction on JAG1-mediated NOTCH1/2 signaling depends on the relative expression levels of JAG1 versus Notch receptors, and that in a $Jag1^{+/-}$ context, decreasing *Poglut1* leads to a net increase in JAG1-mediated signaling, thereby improving the $Jag1^{+/-}$ haploinsufficient liver phenotypes.

ASO-mediated KD in the liver is already employed in clinic to treat several metabolic disorders.[39,40] However, to our knowledge, no ASO-based therapy has been approved

for clinical use in a genetic childhood disease affecting liver development. Our cell-based signaling assays provide strong evidence that the JAG1-expressing, signal-sending cell is the cell type in which *Poglut1* KD promotes biliary development. Previous work has established that the periportal mesenchymal cells are the major source of JAG1 during biliary development.[41] Moreover, our RNAscope analysis indicates that ASO-1 injections lead to efficient KD of *Poglut1* in *Jag1*-expressing periportal mesenchymal cells. Together, these observations strongly suggest that ASO-mediated *Poglut1* KD in periportal mesenchymal cells mediates the observed rescue of the liver phenotypes in our ALGS models. Of note, we previously reported that genetic removal of one copy of *Poglut1* in hepatobiliary cells (*Albumin-Cre*) and periportal mesenchymal cells (*SM22α-Cre*) can both improve the $Jag1^{+/-}$ liver phenotypes,[14] suggesting that the beneficial effects of reducing *Poglut1* in ALGS models are not limited to one cell type. It will remain to be seen whether reducing *Poglut1* specifically in postnatal hepatocytes also contributes to the observed improvement of the ALGS biliary phenotypes upon ASO injections.

Our data provide proof of concept that postnatal targeting of a genetic modifier can improve the liver phenotypes in a pediatric liver disease and establish a framework for developing a therapeutic strategy for ALGS liver disease. However, a number of key issues related to the therapeutic potential of *Poglut1* KD in ALGS remain to be addressed in preclinical models. It is important to examine whether the BDs formed upon ASO injections remain stable beyond P30, and to determine whether ASO injections after the appearance of fibrosis and necrosis are still able to improve the ALGS liver phenotypes. Since ALGS is a multi-system disorder, it is also important to assess whether ASO-mediated *Poglut1* KD can improve other ALGS phenotypes. Finally, given the observed reduction in NOTCH1 and NOTCH2 signaling in $Poglut1^{+/-}$ signal-receiving cells overexpressing these receptors (Fig. 6D), it is critical to ensure that systemic anti-*Poglut1* ASO injections do not negatively affect the cardiovascular system and other organs that depend on NOTCH1 and NOTCH2 signaling.[42]

## Supplementary Material

Refer to Web version on PubMed Central for supplementary material.

## Acknowledgments:

We thank Shakeel Thakurdas for initiating the ASO studies in the Jafar-Nejad laboratory; Joshua Adams for discussions; Bob Haltiwanger for constructs; Shinako Kakuda for advice on Notch signaling assays; Natacha Mitchell, Patricia Castro and Maciej Zelazowski for assistance with the staining and scanning of the H&E slides; and Tom Gridley for the $Jag1^{+/-}$ strain. Image collection for ink injections was performed in the Optical Imaging & Vital Microscopy Core Facility at Baylor College of Medicine. Imaging for liver fibrosis was performed at the Neurovisualization Core Facility at Baylor College of Medicine Intellectual and Developmental Disabilities Research Center. A special thank you to J. Matthew Kofron, CCHMC Confocal Imaging Core Director, for guidance of the RNAscope image analyses. The Graphical Abstract was created with BioRender.com.

**Financial support:**

Supported by the National Institutes of Health (R01 DK109982, R35 GM130317, and R01 AR076770 to H.J.N.; R01 DK120765 and R01 DK107553 to S.S.H.; R01 DK132751 jointly to H.J.N. and S.S.H.); a Pilot/Feasibility Award from the Texas Medical Center Digestive Disease Center to H.J.N. (NIH P30 DK56338); two Alagille Syndrome Accelerator Awards from the Medical Foundation established by generous funding from an anonymous private donor to H.J.N; Funds from the Department of Molecular & Human Genetics, Baylor College of Medicine

to H.J.N.; and T32 GM08307 training grant to D.F; Neurovisualization Core Facility at Baylor College of Medicine Intellectual and Developmental Disabilities Research Center (U54 HD083092); Integrative Morphology Core – Pathology Research Service and Confocal Imaging of the Digestive Diseases Research Core Center in Cincinnati (P30 DK078392). All costs involved in the design, screening and production of ASO-1 was covered by Ionis Pharmaceuticals.

## List of Abbreviations:

| | |
|---|---|
| **ANOVA** | analysis of variance |
| **αSMA** | alpha smooth muscle actin |
| **ASO** | antisense oligonucleotide |
| **ALGS** | Alagille syndrome |
| **BD** | bile duct |
| **cEt** | constrained ethyl |
| **CK** | cytokeratin |
| **H&E** | hematoxylin and eosin |
| **JAG1** | jagged 1 |
| **KD** | knockdown |
| **LGMD** | limb-girdle muscular dystrophy |
| **MEF** | mouse embryonic fibroblast |
| **N1-ICD** | NOTCH1 intracellular domain |
| **OMIM** | Online Mendelian Inheritance in Man |
| **OPN** | osteopontin |
| **PAX7** | paired box 7 |
| **POGLUT1** | protein *O*-glucosyltransferase 1 |
| **PV** | portal vein |
| **qRT-PCR** | quantitative reverse-transcriptase polymerase chain reaction |
| **SOX9** | sex determining region Y-box 9 |
| **SD** | standard deviation |
| **wsCK** | wide-spectrum cytokeratin |
| **WT** | wild-type |

## References


1. Alagille D, Odievre M, Gautier M, Dommergues JP. Hepatic ductular hypoplasia associated with characteristic facies, vertebral malformations, retarded physical, mental, and sexual development, and cardiac murmur. The Journal of pediatrics 1975;86:63–71. [PubMed: 803282]
2. Emerick KM, Rand EB, Goldmuntz E, Krantz ID, Spinner NB, Piccoli DA. Features of Alagille syndrome in 92 patients: frequency and relation to prognosis. Hepatology 1999;29:822–829. [PubMed: 10051485]
3. Li L, Krantz ID, Deng Y, Genin A, Banta AB, Collins CC, et al. Alagille syndrome is caused by mutations in human Jagged1, which encodes a ligand for Notch1. Nature genetics 1997;16:243–251. [PubMed: 9207788]
4. Oda T, Elkahloun AG, Pike BL, Okajima K, Krantz ID, Genin A, et al. Mutations in the human Jagged1 gene are responsible for Alagille syndrome. Nature genetics 1997;16:235–242. [PubMed: 9207787]
5. Warthen DM, Moore EC, Kamath BM, Morrissette JJ, Sanchez-Lara PA, Piccoli DA, et al. Jagged1 (JAG1) mutations in Alagille syndrome: increasing the mutation detection rate. Human mutation 2006;27:436–443. [PubMed: 16575836]
6. Gilbert MA, Bauer RC, Rajagopalan R, Grochowski CM, Chao G, McEldrew D, et al. Alagille syndrome mutation update: Comprehensive overview of JAG1 and NOTCH2 mutation frequencies and insight into missense variant classification. Human mutation 2019;40:2197–2220. [PubMed: 31343788]
7. Kamath BM, Bauer RC, Loomes KM, Chao G, Gerfen J, Hutchinson A, et al. NOTCH2 mutations in Alagille syndrome. Journal of medical genetics 2012;49:138–144. [PubMed: 22209762]
8. McDaniell R, Warthen DM, Sanchez-Lara PA, Pai A, Krantz ID, Piccoli DA, et al. NOTCH2 mutations cause Alagille syndrome, a heterogeneous disorder of the notch signaling pathway. American journal of human genetics 2006;79:169–173. [PubMed: 16773578]
9. Mouzaki M, Bass LM, Sokol RJ, Piccoli DA, Quammie C, Loomes KM, et al. Early life predictive markers of liver disease outcome in an International, Multicentre Cohort of children with Alagille syndrome. Liver international : official journal of the International Association for the Study of the Liver 2016;36:755–760. [PubMed: 26201540]
10. Gonzales E, Hardikar W, Stormon M, Baker A, Hierro L, Gliwicz D, et al. Efficacy and safety of maralixibat treatment in patients with Alagille syndrome and cholestatic pruritus (ICONIC): a randomised phase 2 study. Lancet 2021;398:1581–1592. [PubMed: 34755627]
11. Ayoub MD, Kamath BM. Alagille Syndrome: Diagnostic Challenges and Advances in Management. Diagnostics (Basel) 2020;10:907. [PubMed: 33172025]
12. Kamath BM, Ye W, Goodrich NP, Loomes KM, Romero R, Heubi JE, et al. Outcomes of Childhood Cholestasis in Alagille Syndrome: Results of a Multicenter Observational Study. Hepatology communications 2020;4:387–398. [PubMed: 33313463]
13. Vandriel SM, Li LT, She H, Wang JS, Gilbert MA, Jankowska I, et al. Natural history of liver disease in a large international cohort of children with Alagille syndrome: Results from the GALA study. Hepatology 2023;77:512–529. [PubMed: 36036223]
14. Thakurdas SM, Lopez MF, Kakuda S, Fernandez-Valdivia R, Zarrin-Khameh N, Haltiwanger RS, et al. Jagged1 heterozygosity in mice results in a congenital cholangiopathy which is reversed by concomitant deletion of one copy of Poglut1 (Rumi). Hepatology 2016;63:550–565. [PubMed: 26235536]
15. Adams JM, Huppert KA, Castro EC, Lopez MF, Niknejad N, Subramanian S, et al. Sox9 is a modifier of the liver disease severity in a mouse model of Alagille syndrome. Hepatology 2020;71:1331–1349. [PubMed: 31469182]
16. Xue Y, Gao X, Lindsell CE, Norton CR, Chang B, Hicks C, et al. Embryonic lethality and vascular defects in mice lacking the Notch ligand Jagged1. Human molecular genetics 1999;8:723–730. [PubMed: 10196361]
17. Postic C, Shiota M, Niswender KD, Jetton TL, Chen Y, Moates JM, et al. Dual roles for glucokinase in glucose homeostasis as determined by liver and pancreatic beta cell-specific

gene knock-outs using Cre recombinase. The Journal of biological chemistry 1999;274:305–315. [PubMed: 9867845]

18. Fernandez-Valdivia R, Takeuchi H, Samarghandi A, Lopez M, Leonardi J, Haltiwanger RS, et al. Regulation of mammalian Notch signaling and embryonic development by the protein O-glucosyltransferase Rumi. Development 2011;138:1925–1934. [PubMed: 21490058]
19. Akiyama H, Chaboissier MC, Martin JF, Schedl A, de Crombrugghe B. The transcription factor Sox9 has essential roles in successive steps of the chondrocyte differentiation pathway and is required for expression of Sox5 and Sox6. Genes & development 2002;16:2813–2828. [PubMed: 12414734]
20. Adams JM, Jafar-Nejad H. Determining Bile Duct Density in the Mouse Liver. Journal of visualized experiments : JoVE 2019;146:e59587.
21. Schaub JR, Huppert KA, Kurial SNT, Hsu BY, Cast AE, Donnelly B, et al. De novo formation of the biliary system by TGFbeta-mediated hepatocyte transdifferentiation. Nature 2018;557:247–251. [PubMed: 29720662]
22. Holtwick R, Gotthardt M, Skryabin B, Steinmetz M, Potthast R, Zetsche B, et al. Smooth muscle-selective deletion of guanylyl cyclase-A prevents the acute but not chronic effects of ANP on blood pressure. Proceedings of the National Academy of Sciences of the United States of America 2002;99:7142–7147. [PubMed: 11997476]
23. Wang F, Flanagan J, Su N, Wang LC, Bui S, Nielson A, et al. RNAscope: a novel in situ RNA analysis platform for formalin-fixed, paraffin-embedded tissues. The Journal of molecular diagnostics : JMD 2012;14:22–29. [PubMed: 22166544]
24. Antoniou A, Raynaud P, Cordi S, Zong Y, Tronche F, Stanger BZ, et al. Intrahepatic bile ducts develop according to a new mode of tubulogenesis regulated by the transcription factor SOX9. Gastroenterology 2009;136:2325–2333. [PubMed: 19403103]
25. Servian-Morilla E, Takeuchi H, Lee TV, Clarimon J, Mavillard F, Area-Gomez E, et al. A POGLUT1 mutation causes a muscular dystrophy with reduced Notch signaling and satellite cell loss. EMBO molecular medicine 2016;8:1289–1309. [PubMed: 27807076]
26. Servian-Morilla E, Cabrera-Serrano M, Johnson K, Pandey A, Ito A, Rivas E, et al. POGLUT1 biallelic mutations cause myopathy with reduced satellite cells, alpha-dystroglycan hypoglycosylation and a distinctive radiological pattern. Acta Neuropathol 2020;139:565–582. [PubMed: 31897643]
27. Rana NA, Nita-Lazar A, Takeuchi H, Kakuda S, Luther KB, Haltiwanger RS. O-glucose trisaccharide is present at high but variable stoichiometry at multiple sites on mouse Notch1. The Journal of biological chemistry 2011;286:31623–31637. [PubMed: 21757702]
28. Kakuda S, Haltiwanger RS. Deciphering the Fringe-Mediated Notch Code: Identification of Activating and Inhibiting Sites Allowing Discrimination between Ligands. Developmental cell 2017;40:193–201. [PubMed: 28089369]
29. Meena BL, Khanna R, Bihari C, Rastogi A, Rawat D, Alam S. Bile duct paucity in childhood-spectrum, profile, and outcome. Eur J Pediatr 2018;177:1261–1269. [PubMed: 29868931]
30. Shneider BL, Spino CA, Kamath BM, Magee JC, Ignacio RV, Huang S, et al. Impact of long-term administration of maralixibat on children with cholestasis secondary to Alagille syndrome. Hepatology communications 2022;6:1922–1933. [PubMed: 35672955]
31. Loomes KM, Squires RH, Kelly D, Rajwal S, Soufi N, Lachaux A, et al. Maralixibat for the treatment of PFIC: Long-term, IBAT inhibition in an open-label, Phase 2 study. Hepatology communications 2022;6:2379–2390. [PubMed: 35507739]
32. Zhao C, Matalonga J, Lancman JJ, Liu L, Xiao C, Kumar S, et al. Regenerative failure of intrahepatic biliary cells in Alagille syndrome rescued by elevated Jagged/Notch/Sox9 signaling. Proceedings of the National Academy of Sciences of the United States of America 2022;119:e2201097119. [PubMed: 36469766]
33. Zong Y, Panikkar A, Xu J, Antoniou A, Raynaud P, Lemaigre F, et al. Notch signaling controls liver development by regulating biliary differentiation. Development 2009;136:1727–1739. [PubMed: 19369401]

34. Poncy A, Antoniou A, Cordi S, Pierreux CE, Jacquemin P, Lemaigre FP. Transcription factors SOX4 and SOX9 cooperatively control development of bile ducts. Developmental biology 2015;404:136–148. [PubMed: 26033091]

35. Tulasi DY, Castaneda DM, Wager K, Hogan CB, Alcedo KP, Raab JR, et al. Sox9(EGFP) Defines Biliary Epithelial Heterogeneity Downstream of Yap Activity. Cellular and molecular gastroenterology and hepatology 2021;11:1437–1462. [PubMed: 33497866]

36. Acar M, Jafar-Nejad H, Takeuchi H, Rajan A, Ibrani D, Rana NA, et al. Rumi is a CAP10 domain glycosyltransferase that modifies Notch and is required for Notch signaling. Cell 2008;132:247–258. [PubMed: 18243100]

37. Leonardi J, Fernandez-Valdivia R, Li YD, Simcox AA, Jafar-Nejad H. Multiple O-glucosylation sites on Notch function as a buffer against temperature-dependent loss of signaling. Development 2011;138:3569–3578. [PubMed: 21771811]

38. Pandey A, Niknejad N, Jafar-Nejad H. Multifaceted regulation of Notch signaling by glycosylation. Glycobiology 2021;31:8–28. [PubMed: 32472127]

39. Raal FJ, Santos RD, Blom DJ, Marais AD, Charng MJ, Cromwell WC, et al. Mipomersen, an apolipoprotein B synthesis inhibitor, for lowering of LDL cholesterol concentrations in patients with homozygous familial hypercholesterolaemia: a randomised, double-blind, placebo-controlled trial. Lancet 2010;375:998–1006. [PubMed: 20227758]

40. Witztum JL, Gaudet D, Freedman SD, Alexander VJ, Digenio A, Williams KR, et al. Volanesorsen and Triglyceride Levels in Familial Chylomicronemia Syndrome. The New England journal of medicine 2019;381:531–542. [PubMed: 31390500]

41. Hofmann JJ, Zovein AC, Koh H, Radtke F, Weinmaster G, Iruela-Arispe ML. Jagged1 in the portal vein mesenchyme regulates intrahepatic bile duct development: insights into Alagille syndrome. Development 2010;137:4061–4072. [PubMed: 21062863]

42. Masek J, Andersson ER. The developmental biology of genetic Notch disorders. Development 2017;144:1743–1763. [PubMed: 28512196]

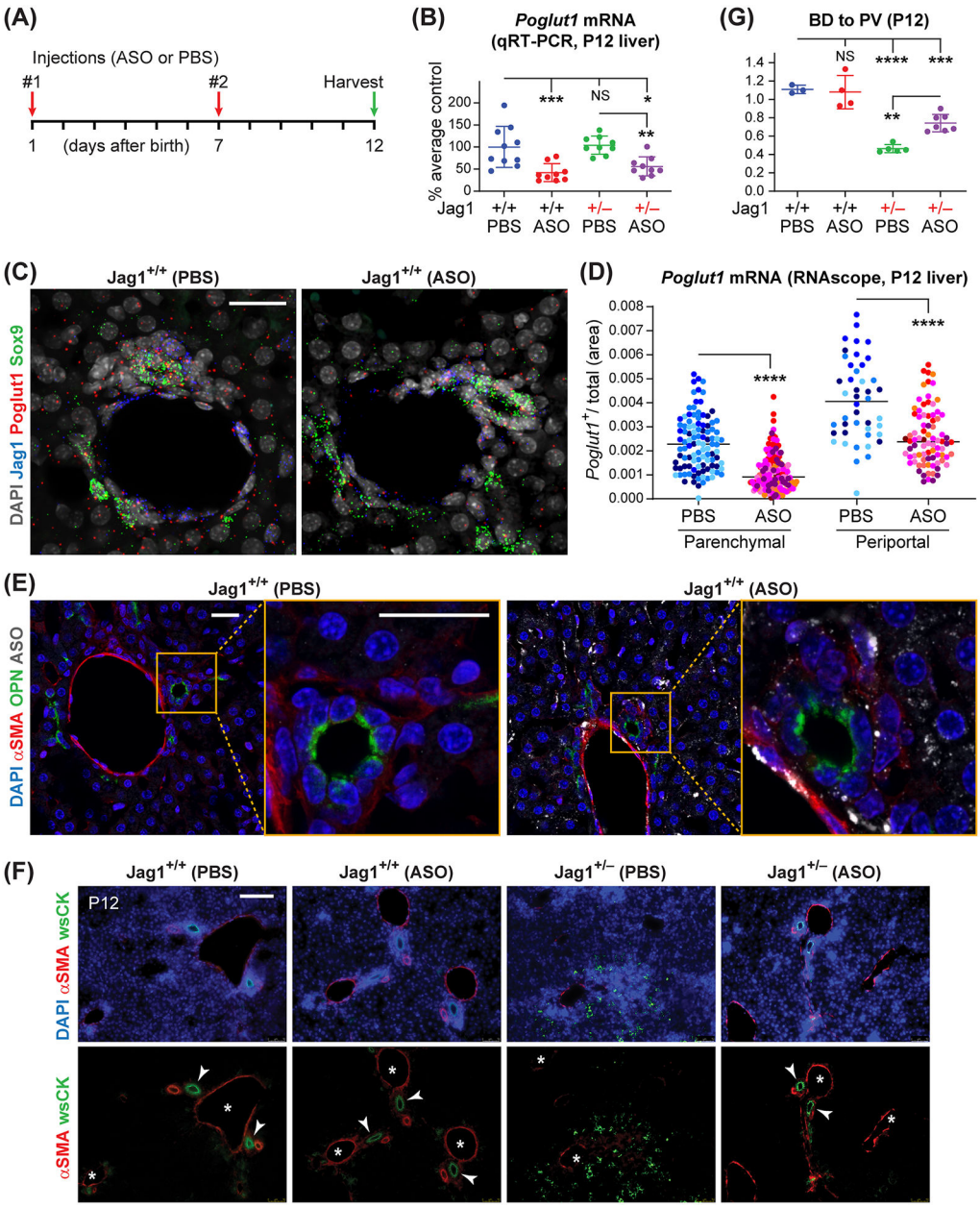


**Fig. 1. Early postnatal injection of ASO-1 broadly knocks down *Poglut1* in the liver and partially rescues the biliary abnormalities in P12 *Jag1*$^{+/-}$ animals.**

(A) Injection regimen of ASO-1 and PBS in *Jag1*$^{+/-}$ and WT animals (50 mg/kg/dose). (B) qRT-PCR assays for *Poglut1* mRNA levels on WT and *Jag1*$^{+/-}$ P12 livers injected with ASO or PBS. (C) Liver RNAscope images from ASO- or PBS-injected P12 WT animals, labeled with DAPI and probes for *Poglut1*, *Sox9*, and *Jag1*. (D) Quantification of relative *Poglut1*$^{+}$ area of RNAscope images in parenchymal and periportal regions. (E) Liver sections from ASO- or PBS-injected P12 WT animals, stained with antibodies against ASO, osteopontin (OPN) and αSMA. (F) P12 liver sections of each genotype stained with αSMA, wide-spectrum cytokeratin (wsCK) and DAPI. Asterisks mark PVs, arrowheads mark patent BDs. Note the weak αSMA staining, ductular reactions and hypercellularity

in the parenchyma of PBS-injected *Jag1*$^{+/-}$ livers and their rescue upon ASO injections. (G) Average BD to PV ratio in P12 WT and *Jag1*$^{+/-}$ mice injected with PBS or ASO. In B and G, each circle represents an animal and horizontal lines show mean ± Standard Deviation (SD). In D, circles of the same color represent data from different parenchymal or periportal regions of liver sections from the same animal (n=4 for PBS-injected, n=7 for ASO-injected). NS: not significant, **P*<0.05, ***P*<0.01, ****P*<0.001, *****P*<0.0001, using one-way ANOVA with Tukey's multiple comparisons test (B, G) or unpaired t-test with Welch's correction (D). Scale bars are 25 μm in C, E, and 100 μm in F.

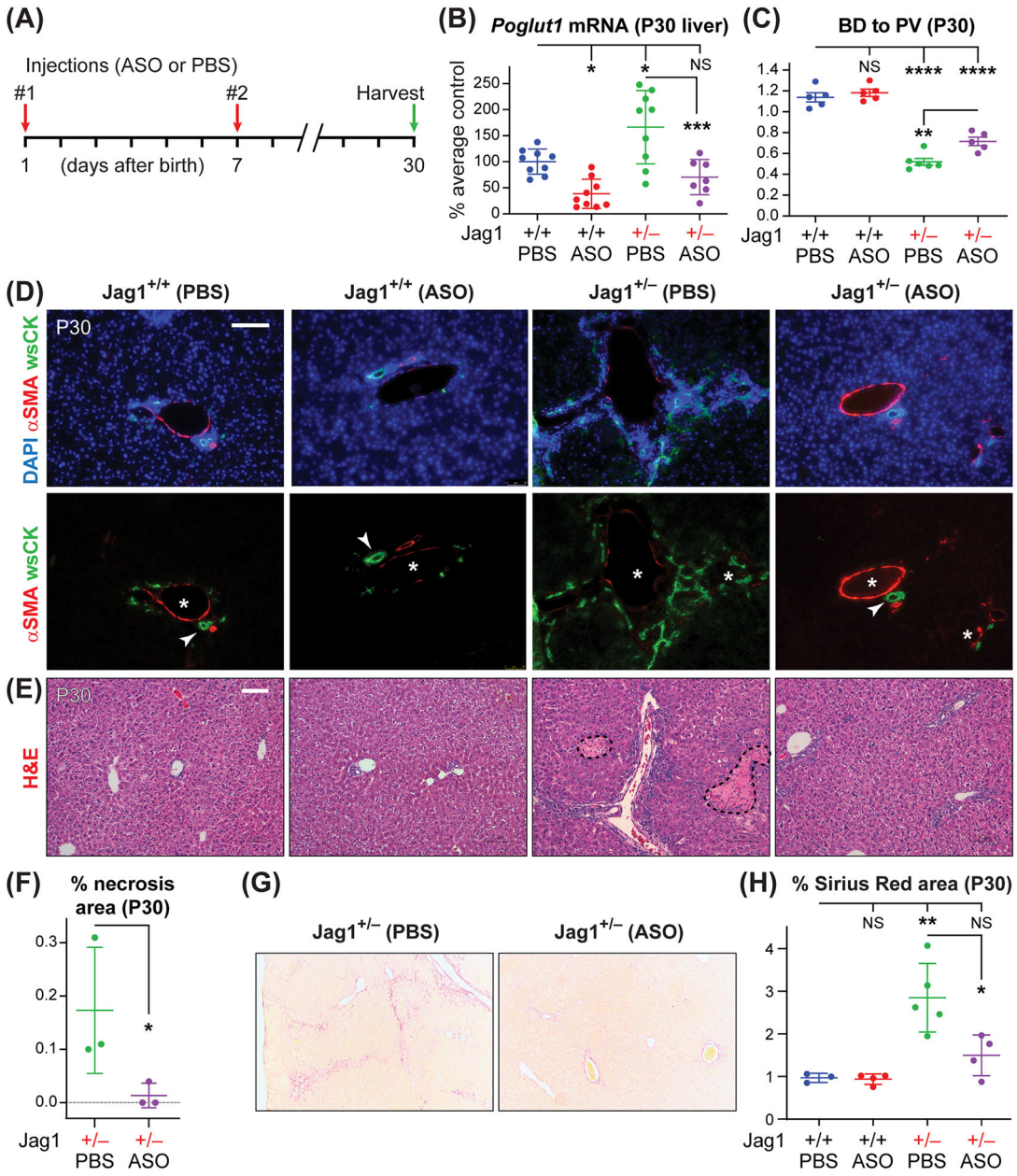


**Fig. 2. *Poglut1* KD in early postnatal period improves biliary development and significantly decreases liver damage in P30 *Jag1*$^{+/-}$ mice.**

(**A**) Injection regimen of ASO-1 and PBS in *Jag1*$^{+/-}$ and WT animals (50 mg/kg/dose). (**B**) qRT-PCR assays for *Poglut1* mRNA levels on WT and *Jag1*$^{+/-}$ P30 livers injected with ASO or PBS. Note the increase in the *Poglut1* mRNA levels in *Jag1*$^{+/-}$ livers compared to WT livers at this age. (**C**) Average BD to PV ratio in P30 WT and *Jag1*$^{+/-}$ mice injected with PBS or ASO. (**D**) P30 liver sections of each genotype stained with αSMA, wide-spectrum cytokeratin (wsCK) and DAPI. Asterisks mark PVs, arrowheads mark patent BDs. ASO-1 partially rescues the BD to PV ratio in *Jag1*$^{+/-}$ animals and reduces the ductular reactions and parenchymal hypercellularity observed in control animals. (**E**) Hematoxylin and eosin (H&E) staining of P30 liver sections from the indicated genotypes. Dashed shapes mark

areas of necrosis. (**F**) Percent area of necrotic regions in H&E staining of liver sections form ASO- and PBS-injected animals. (**G**) Sirius Red staining of P30 livers from *Jag1*$^{+/-}$ animals injected with ASO-1 or PBS. (**H**) The degree of liver fibrosis in the indicated genotypes are measured as the percent area of each liver stained with Sirius Red. In **B**, **C**, **F** and **H**, each circle represents an animal and horizontal lines show mean ± SD. NS: not significant, **P*<0.05, ***P*<0.01, ****P*<0.001, *****P*<0.0001, using one-way ANOVA with Tukey's multiple comparisons test (**B**, **C**, **H**) or unpaired t-test (**F**). Scale bars are 100 μm.

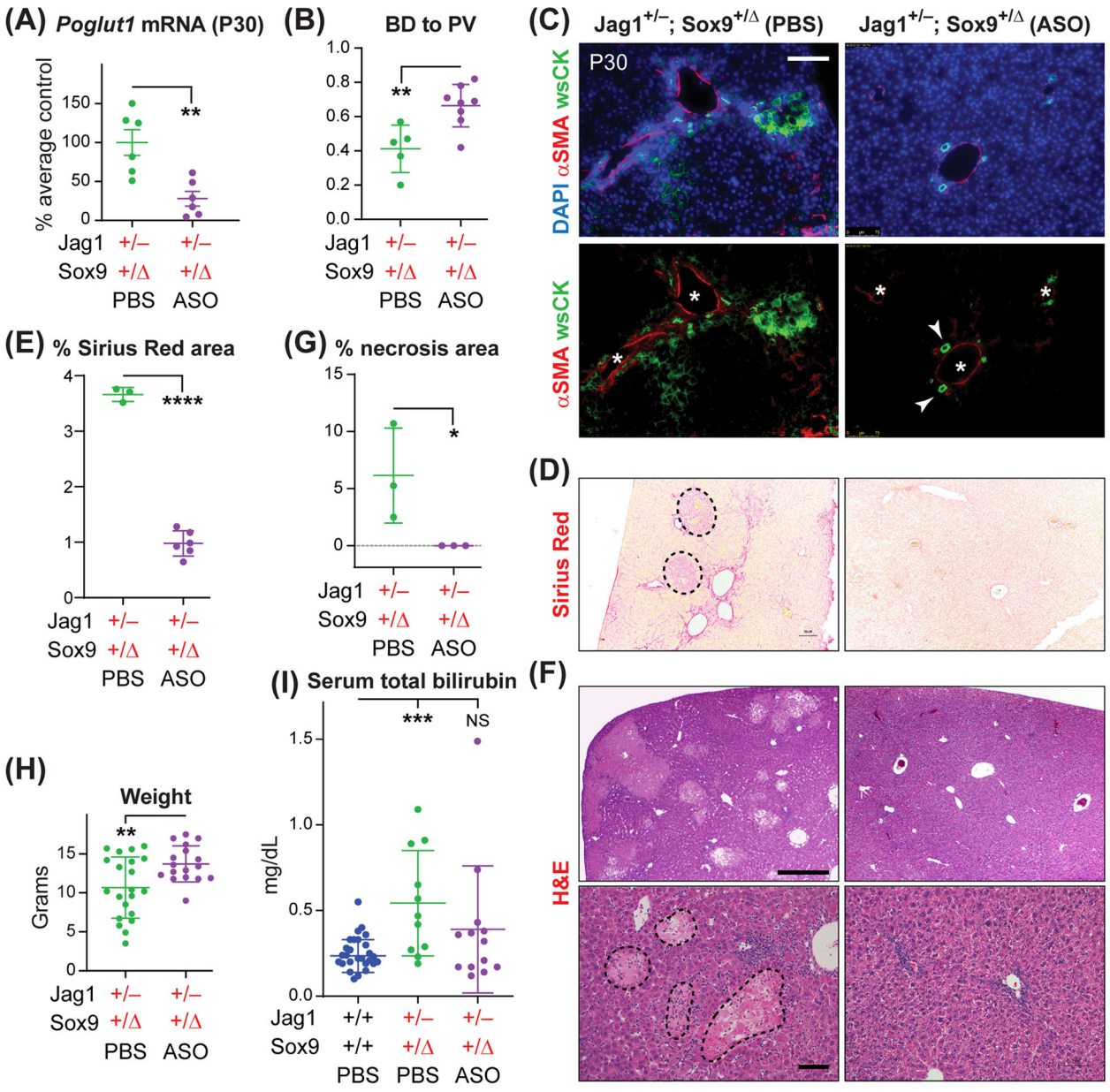


**Fig. 3. ASO-1 injections improve the liver phenotypes in *Jag1*$^{+/-}$ animals lacking one copy of *Sox9* in the liver.**

(**A**) qRT-PCR assays for *Poglut1* mRNA levels on *Jag1*$^{+/-}$;*Sox9*$^{+/\Delta}$ P30 livers injected with ASO or PBS. (**B**) Average BD to PV ratio in *Jag1*$^{+/-}$;*Sox9*$^{+/\Delta}$ mice injected with PBS or ASO. (**C**) P30 liver sections of each genotype stained with αSMA, wide-spectrum cytokeratin (wsCK) and DAPI. Asterisks mark PVs, arrowheads mark patent BDs. Scale bar is 100 μm. (**D**) Sirius Red staining of P30 livers from *Jag1*$^{+/-}$;*Sox9*$^{+/\Delta}$ animals injected with ASO-1 or PBS. Necrotic regions (dashed shapes) were excluded from quantification. (**E**) The degree of liver fibrosis in the indicated genotypes are measured as the percent area of each liver stained with Sirius Red. (**F**) H&E staining of P30 liver sections from *Jag1*$^{+/-}$;*Sox9*$^{+/\Delta}$ animals injected with ASO-1 or PBS. Dashed shapes in the lower-left panel

mark areas of necrosis. Scale bars are 500 μm (top panels) and 100 μm (bottom panels). (**G**) Percent area of necrotic regions in H&E staining of liver sections form the indicated genotypes. (**H**) Weights for P30 *Jag1*$^{+/-}$;*Sox9*$^{+/\Delta}$ animals injected with ASO-1 or PBS. (**I**), Serum total bilirubin for the indicated genotypes. In all graphs, each circle represents an animal and horizontal lines show mean ± SD. NS: not significant, **P*<0.05, ***P*<0.01, ****P*<0.001, *****P*<0.0001, using one-way ANOVA with Tukey's multiple comparisons test (**I**) or unpaired t-test (**A**, **B**, **E**, **G**, **H**).

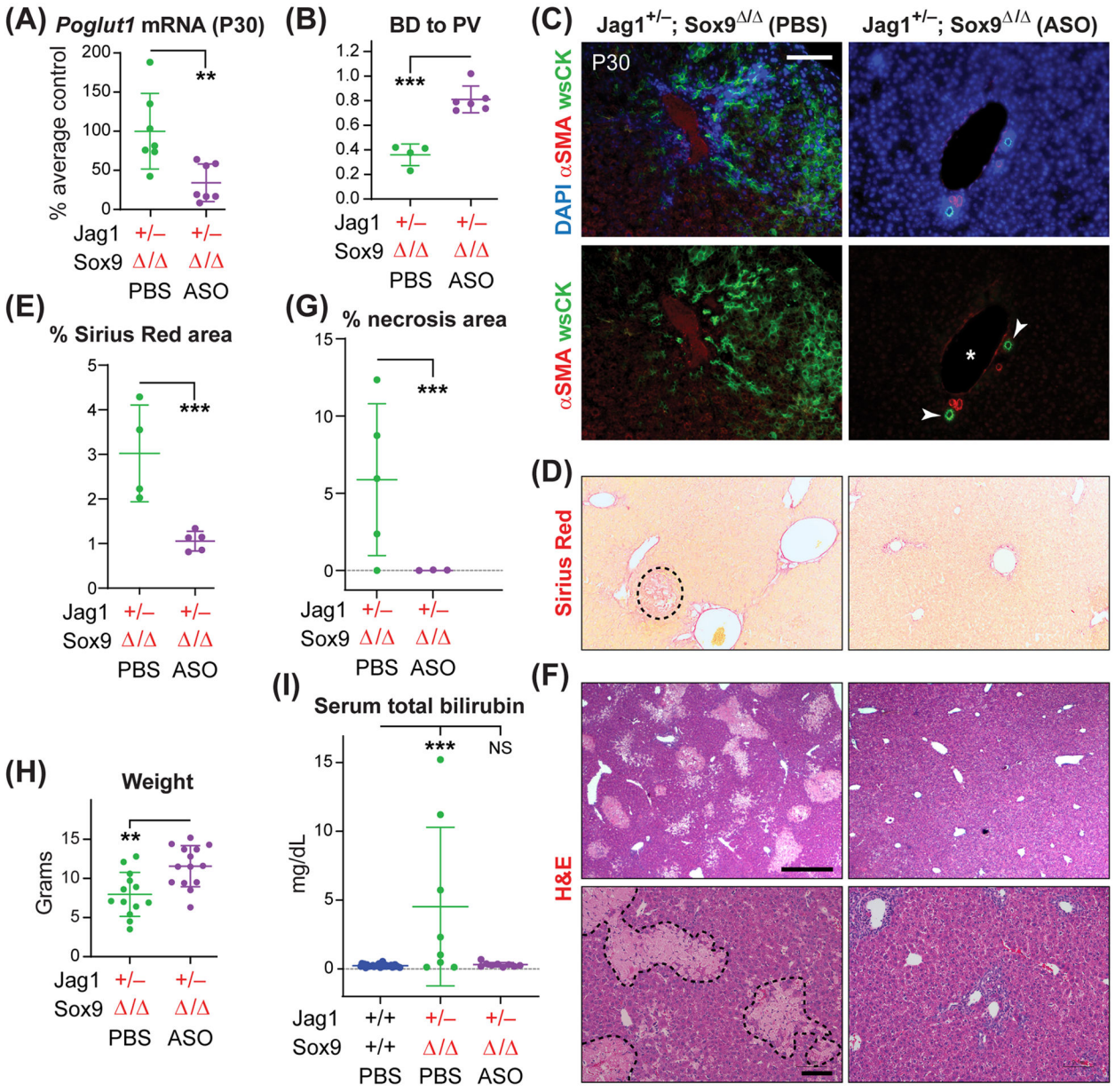


**Fig. 4. ASO-1 injections improve the liver phenotypes in *Jag1*$^{+/-}$ animals lacking both copies of *Sox9* in the liver.**

(**A**) qRT-PCR assays for *Poglut1* mRNA levels on *Jag1*$^{+/-}$;*Sox9*$^{\Delta/\Delta}$ P30 livers injected with ASO or PBS. (**B**) Average BD to PV ratio in *Jag1*$^{+/-}$;*Sox9*$^{\Delta/\Delta}$ mice injected with PBS or ASO. (**C**) P30 liver sections of each genotype stained with αSMA, wide-spectrum cytokeratin (wsCK) and DAPI. Asterisks mark PVs, arrowheads mark patent BDs. Scale bar is 100 μm. (**D**) Sirius Red staining of P30 livers from *Jag1*$^{+/-}$;*Sox9*$^{\Delta/\Delta}$ animals injected with ASO or PBS. The dashed shape marks a necrotic region. (**E**) The degrees of liver fibrosis in the indicated genotypes are measured as the percent area of each liver stained with Sirius Red. (**F**) H&E staining of P30 liver sections from *Jag1*$^{+/-}$;*Sox9*$^{\Delta/\Delta}$ animals injected with ASO or PBS. Dashed shapes in the lower-left panel mark areas of necrosis. Scale bars are 500 μm (top panels) and 100 μm (bottom panels). Note that some degree of periportal

inflammation persists in ASO-injected livers. (**G**) Percent area of necrotic regions in H&E staining of liver sections form the indicated genotypes. (**H**) Weights for P30 *Jag1*$^{+/-}$;*Sox9*$^{\Delta/\Delta}$ animals injected with ASO or PBS. (**I**) Serum total bilirubin for the indicated genotypes. In all graphs, each circle represents an animal and horizontal lines show mean ± SD. NS: not significant, ** $P<0.01$, *** $P<0.001$, using one-way ANOVA with Tukey's multiple comparisons test (**I**) or unpaired t-test (**A**, **B**, **E**, **G**, **H**).

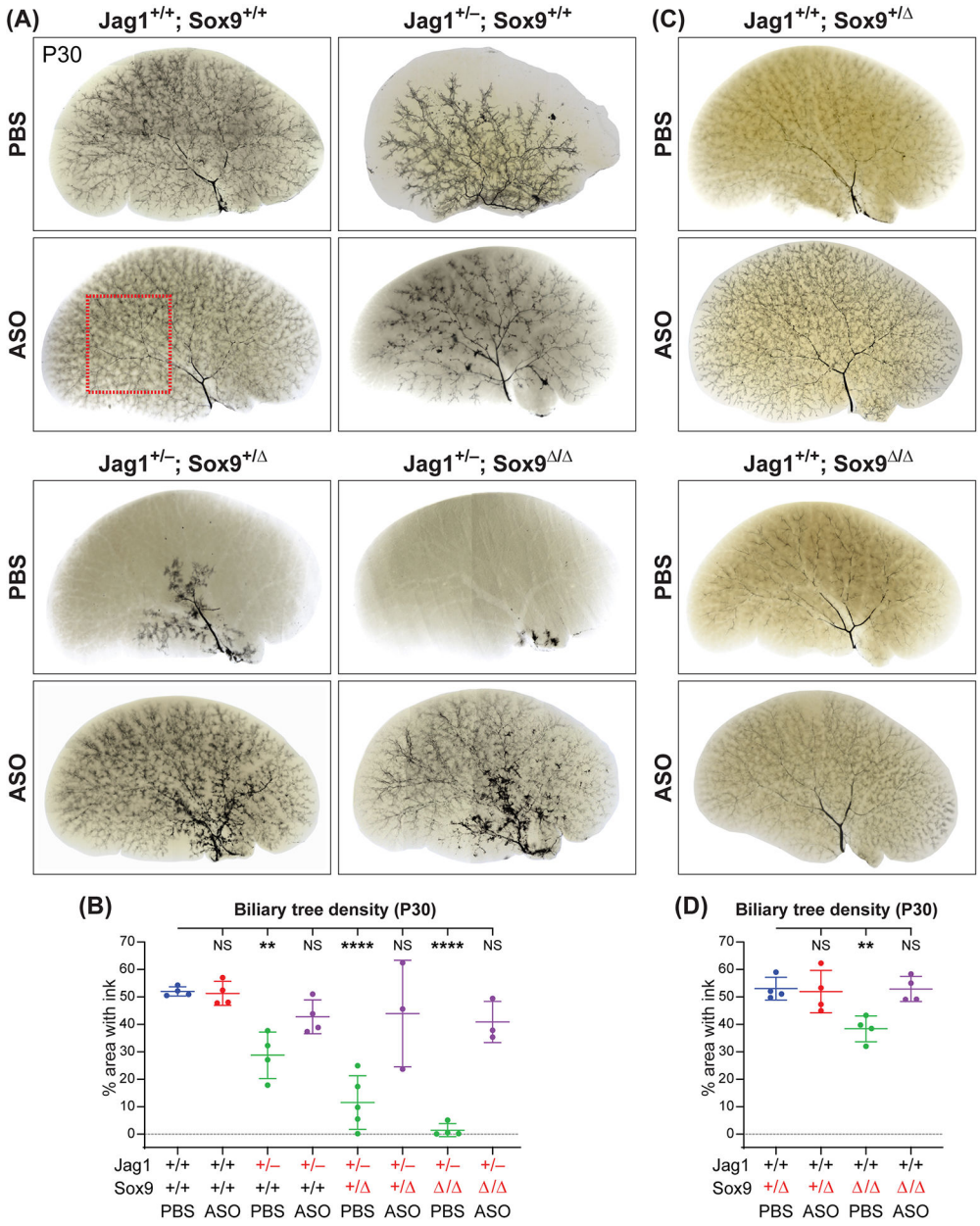


**Fig. 5. ASO-1 injections result in a dramatic improvement in the biliary tree structure of ALGS models.**

(**A, C**) Ink injection images of the left liver lobes of P30 animals with indicated genotypes injected with two doses of ASO-1 or PBS. Each image is representative of 3–5 animals for each condition. The pale structures in the liver parenchyma mark the outline of portal veins and are easier to see in the absence of the biliary tree. (**B, D)** Quantification of the percent area covered by the ink-filled biliary tree in a flattened image of each left liver lobe. The red dashed box in **A** indicates the area used for quantification of the biliary tree density except in PBS-injected *Jag1*$^{+/-}$;*Sox9*$^{+/\Delta}$ and *Jag1*$^{+/-}$;*Sox9*$^{\Delta/\Delta}$ livers, where the red dashed box was placed over the hilar region to maximize the ink-filled area used in quantification. Each circle represents an animal and horizontal lines show mean ± SD. NS: not significant,

** $P<0.01$, **** $P<0.0001$, using one-way ANOVA with Dunnett's multiple comparisons test.

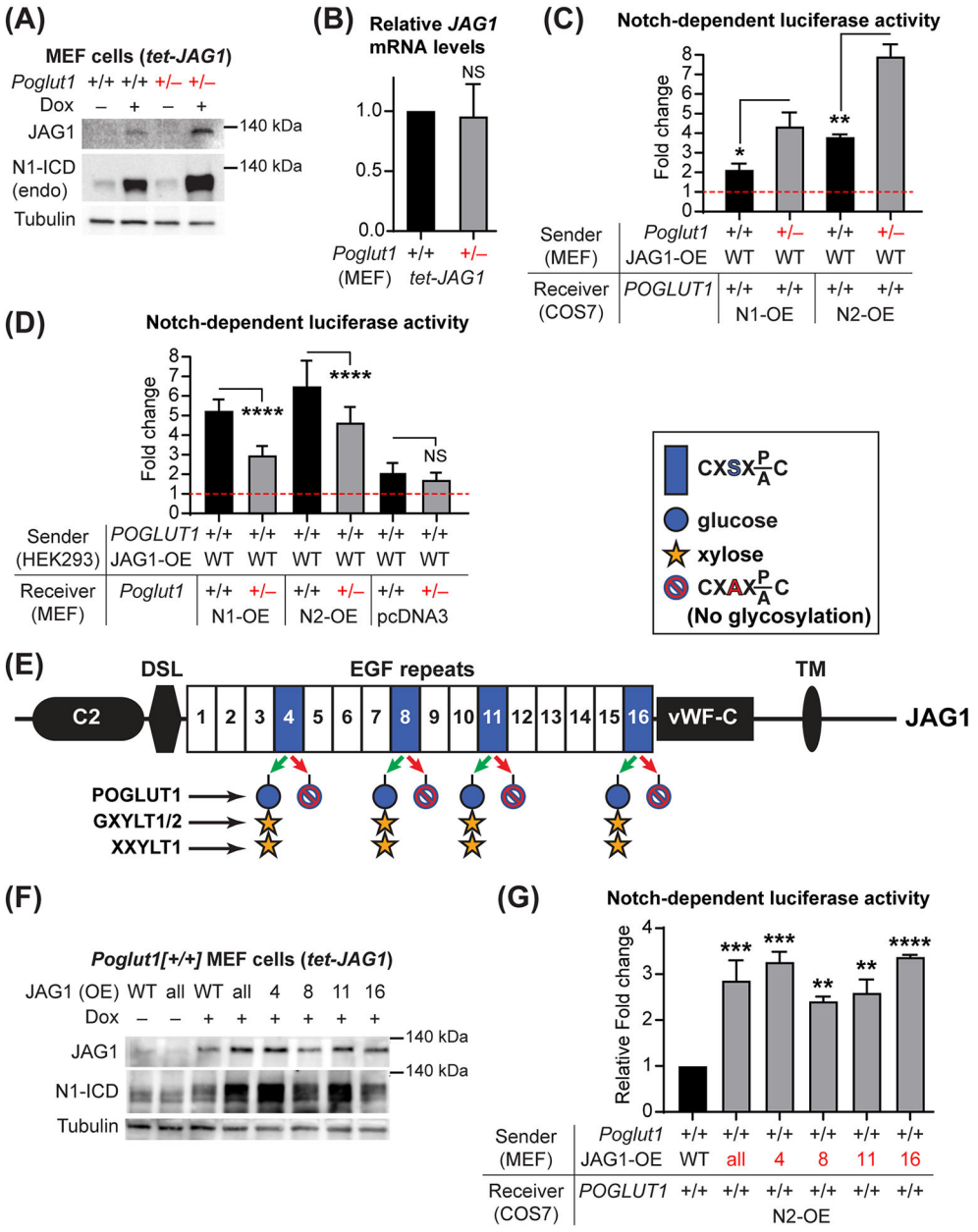


**Fig. 6. POGLUT1 negatively regulates JAG1 protein level and JAG1-mediated signaling.**

(**A**) Immunoblots with anti-JAG1, anti-cleaved NOTCH1 intracellular domain (N1-ICD) and anti-Tubulin (loading control) antibodies are shown for WT and *Poglut1*$^{+/-}$ MEFs with or without doxycycline (Dox) induction of human *JAG1* expression. Data are representative of 3 independent experiments. endo: endogenous. (**B**) qRT-PCR assays for human *JAG1* mRNA in WT and *Poglut1*$^{+/-}$ MEFs treated with Dox to induce human *JAG1* expression. (**C**) Co-culture signaling assays between WT or *Poglut1*$^{+/-}$ MEFs with or without human *JAG1* overexpression and *POGLUT1*$^{+/+}$ COS7 cells overexpressing NOTCH1 (N1-OE) or NOTCH2 (N2-OE) along with the TP1–1-luciferase construct. For each co-culture, the fold change of luciferase induction upon Dox-induced expression of human JAG1 compared to the same co-culture without human JAG1 induction (red line set at 1) is shown. (**D**)

Fold change of Notch-dependent luciferase induction upon human JAG1 expression is shown for the indicated co-culture conditions. (**E**) Schematic of the human JAG1 protein. Blue boxes show EGF repeats with a POGLUT1 target site, along with the trisaccharide and the enzymes responsible for its formation. C2, phospholipid recognition; DSL, Delta-Serrate-Lag2; vWF-C, von Willebrand factor type C; TM, transmembrane. S-to-A mutations prevent *O*-glucosylation by POGLUT1. (**F**) Immunoblots for WT cells with or without Dox induction of human JAG1 (WT or harboring S-to-A mutations in individual or all POGLUT1 target sites). Data are representative of 4 independent experiments. (**G**) Co-culture signaling assays to assess the impact of the POGLUT1 target site mutations on the ability of JAG1 to induce NOTCH2 signaling in neighboring cells. Signaling induced by WT JAG1 was set to 1; signaling by mutant JAG1 proteins are shown as relative fold change compared to that induced by WT JAG1. In **C**, **D** and **G**, n=9 for each column. Each graph shows the results from a representative experiment from 3–4 independent experiments. In **B**, n=4 for each column. In all graphs, mean + SD is shown. NS: not significant, **P*<0.05, ***P*<0.01, ****P*<0.001, *****P*<0.0001, using one-way ANOVA with Tukey's multiple comparisons test (**D**, **G**) or unpaired t-test (**B**, **C**).